Available online at www.sciencedirect.com
ScienceDirect
Journal of the European Ceramic Society 28 (2008) 1793–1799
www.elsevier.com/locate/jeurceramsoc

Lowering the sintering temperature for EPD coatings by applying reaction bonding

Bernd Baufeld [a,*], Omer van der Biest [a], Hans-Joachim Rätzer-Scheibe [b]

[a] *Metaalkunde en Toegepaste Materiaalkunde, Katholieke Universiteit Leuven, Kasteelpark Arenberg 44, 3001 Leuven, Belgium*
[b] *Institute of Materials Research, German Aerospace Center (DLR), Linder Höhe, 51147 Cologne, Germany*

Received 30 August 2007; received in revised form 7 November 2007; accepted 16 November 2007
Available online 4 March 2008

Abstract

Electrophoretic deposition (EPD) allows the fabrication of ceramic coatings, for example of thermal barrier coatings for turbine engines, at lower cost and higher speed than most other deposition techniques. The commonly used sintering temperatures of more than 1200 °C however may damage the metal parts and also lead to high production costs.

This study suggests a powder mixture of zirconia and zirconium nitride to lower the sintering temperature, where during sintering in air at 1000 °C a homogenous, porous zirconia coating was obtained. The thermal conductivity determined by laser flash experiments proved to be significantly lower than that of conventional thermal barrier coatings.

Keywords: Suspension; Electrophoretic deposition; Porosity; Thermal conductivity; ZrO_2

1. Introduction

Ceramic coatings are widely applied for example as protection against wear, corrosion, and oxidation or as thermal barrier coatings in turbine engines. More specifically, yttria-stabilized zirconia (YSZ) is frequently used for these purposes due to its excellent mechanical properties such as high bending strength and fracture toughness. These properties are related to different toughening processes like tetragonal-monoclinic transformation[1] and ferroelasticity.[2–4] Common coating techniques are for example plasma spraying, chemical and physical vapour deposition, which work well but may be rather cost and time intensive. Electrophoretic deposition (EPD) on the other side allows the fabrication of ceramic coatings at lower cost and higher speed than most other deposition techniques.[5–8] EPD implies the deposition of powder from a suspension under the influence of an electric field and the subsequent consolidation by sintering. Commonly the sintering temperatures are in the order of 1200 °C and higher.[6,8] These high temperatures are one of the main disadvantages of applying EPD for the fabrication of ceramic coatings since they easily may damage metal substrates and metal coatings. Furthermore, high sintering temperatures mean also high production cost. Therefore EPD methods allowing lower temperatures may have a significant commercial value.

In order to overcome this disadvantage of high sinter temperatures, reaction bonding is studied. Reaction bonding already was applied by Wang et al.[6,9] for EPD coatings derived from a suspension with 3 mol% Y_2O_3 stabilized ZrO_2 and Al powder. Due to the volume expansion during the oxidation of Al a dense ZrO_2/Al_2O_3 coating was obtained. However, the applied sinter temperature was between 1150 and 1300 °C. Furthermore, for certain applications ZrO_2/Al_2O_3 may not be ideal and pure ZrO2 would be preferable. Another potential candidate for reaction bonding is ZrN due to its low reaction temperature. For example, it is reported that ZrN coatings degrade in air at temperatures higher than 500 °C.[10] A zirconia/ZrN suspension was already employed successfully for the fabrication of an environmental protection coating for a ceramic/ceramic matrix component applied by dip coating.[11] The applied sintering temperature, however, was 1300 °C. Therefore, in the present paper the applicability of a zirconia/ZrN suspension for EPD with a lower sintering temperature of 1000 °C will be studied. Furthermore, the thermal conductivity of the ceramic coating will be determined by the laser flash technique.

* Corresponding author. Tel.: +32 16321534; fax: +32 16321992.
E-mail address: bernd.baufeld@mtm.kuleuven.be (B. Baufeld).

0955-2219/$ – see front matter © 2008 Elsevier Ltd. All rights reserved.
doi:10.1016/j.jeurceramsoc.2007.11.019

Table 1
Composition of the ethanol suspensions

Suspension name		*A*	*B*	*C*
Powder fractions	Zirconia	90.2 wt%	82.6 wt%	99.2 wt%
	CoO	0.7 wt%	0.6 wt%	0.8 wt%
	ZrN	9.1 wt%	16.8 wt%	0
Suspension stabilizers	*n*-Butylamine		3 vol.%	
	Dolapix CE64		1 wt%	
Powder load			96 g/l	

2. Experimental

2.1. Specimen preparation

YSZ (Melox 5Y XZO 99.8%, i.e. 5 mol% Y_2O_3), cobalt oxide as a sintering aid[12] (Aldrich cobalt(II, III)oxide 99.8%), and ZrN (ZR-501, 99.8% ZrN, Atlantis Equipment Engineers) were used. Since the grain size of the ZrN powder is rather large (1–5 μm according to the supplier), the ZrN powder was first ball milled with zirconia balls in ethanol for 1 day. Then the zirconia and the CoO powders were added and everything was ball milled again for 1 day. Two different compositions were investigated (see Table 1), i.e. one with 9.1 (*A*) and one with 16.8 wt% ZrN (*B*). For comparison, a third type of suspension *C* was prepared under similar conditions, but without the addition of ZrN.[13] The suspension was prepared by adding *n*-butylamine (BA) and Dolapix CE64 as suspension stabilization additives (see Table 1) to the powder/ethanol slurry. The suspension was first stirred mechanically, then ultrasonically, and finally again mechanically (15 min each sequence).

Two different substrate types were used. One consisted of the Ni based superalloy IN600 and a rather rough and porous plasma sprayed NiCoCrAlY coating. In order to reduce the original roughness the metal coating has been grinded down to a thickness to about 0.1 mm. The other substrate type, used for the laser flash technique, is called quasi-free-standing coating,[14] and will be described in the following paragraph in detail.

The EPD cell consisted of a non-conductive container and two electrodes, where one of them was the substrate. During EPD, the suspension was subjected to further mechanical stirring. The experimental conditions and data of the laser flash specimens are presented in Table 2. The yield from suspensions *A* and *B* is comparable and increases with deposition time (Fig. 1). The drying in ambient conditions was followed by heat treatment for 6 h: specimens from suspensions *A* and *B* in air at 1000 °C and specimen from suspension *C* in hydrogen atmosphere at 1200 °C.

Table 2
EPD conditions and data of the laser flash specimens (for the porosity calculation the density of 6.05 g/cm^3 is assumed for fully dense zirconia)

Specimens from suspension	*A*	*B*	*C*
Electrical field strength (V/mm)		2.8	
Electrical current (mA)	36	45	38
EPD time (s)	90	90	120
EPD thickness (mm)	0.11	0.09	0.10
Density (g/cm^3)	2.5	3.3	3.7
Porosity (%)	59	46	38

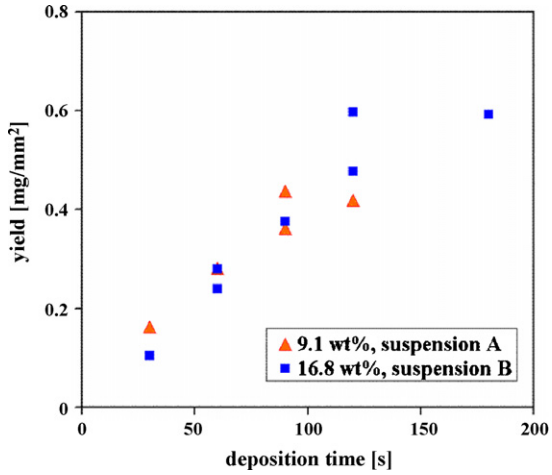

Fig. 1. Ceramic yield of the green coating derived from suspensions *A* and *B* in dependence on the deposition time.

The green coatings from suspensions *A* and *B* have finely grained zirconia and coarser ZrN grains (Fig. 2). They have a dark grey colour, which is related to the black ZrN powder and turn white during heat treatment in air. Heat treatment of specimens with thicker coatings resulted in extensive spallation, limiting the final thickness of adherent EPD coatings to about 0.1 mm. Fig. 3 shows the fracture side of a spalled EPD coating. From the microstructure it is obvious that despite the relatively low temperature sintering took place. In comparison with the green coating (Fig. 2) the very fine grains disappeared and the grains developed a round appearance. The obtained ceramic coating is rather porous, which agrees with density calculations using the mass change due to EPD and the specimen geometry (Table 2). On the fracture surface of the EPD spalls one can not only observe the round zirconia grains, but also frequently larger grains with straight edges, which can be identified with the help of energy dispersive X-ray analysis as Cr and Co con-

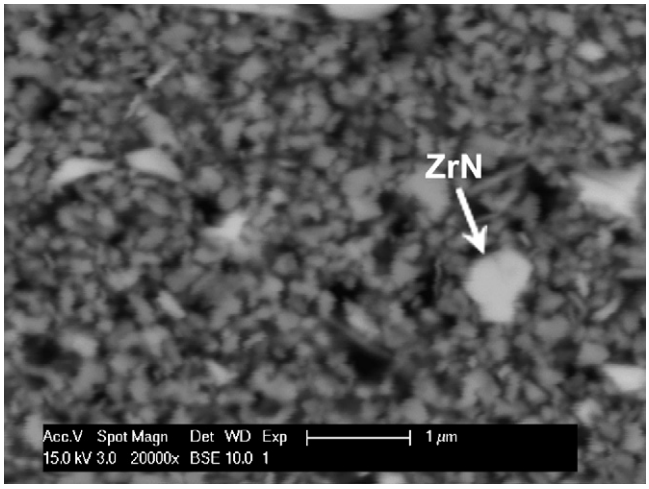

Fig. 2. Back-scattered secondary electron micrograph of a green coating from suspension *B* showing the finely grained YSZ and the larger ZrN grains (brighter contrast).

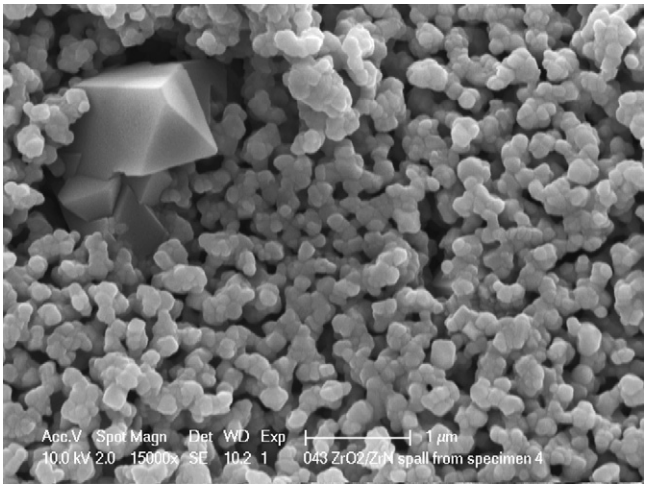

Fig. 3. Spall surface from a sintered EPD coating derived from suspension *A*, viewed from the fracture side.

taining oxides. These are thermally grown oxides (TGO) which develop during heat treatment in air at the interface between the NiCoCrAlY coating and the ceramic EPD layer. NiCoCrAlY coatings are designed to form a dense alumina TGO, but in case of a local Al deficiency, possibly attributed to the porosity of the plasma sprayed metal coating, also Co and Cr will oxidize.

2.2. Characterisation techniques

The thermal diffusivity of the EPD coating was measured using the laser flash method (LFA427, NETZSCH). In this technique, the front side of a plan-parallel disk is heated by a short laser pulse (neodymium doped gallium gadolinium garnet laser with a wavelength of 1.064 μm). The heat diffuses through the sample and the resulting temperature rise of the rear surface is recorded by an infrared detector (2–5 μm wavelength range). The thermal diffusivity is determined from the measured temperature rise and analyzed by the NETZSCH LFA Proteus® software. Thermal conductivity of the coating k is then calculated using the relationship $k = c_p \rho \alpha$, where c_p is the temperature dependent specific heat,[15] ρ the density, and α is the thermal diffusivity. The analysis is based on a one-dimensional heat flow and takes the heat loss from all surfaces of the disk-shaped sample into account. In contrast to former analyses,[14] the effect of the radiative heat transfer in the interior of the sample, which is especially noticeable at higher temperatures,[16] is considered by this software.

A special sample type called quasi-free-standing coating allows measuring the thermal conductivity of fragile and thin coatings. This sample type consists of a sapphire support (diameter 12.7 mm, thickness 1 mm) on which the ceramic EPD coating is deposited. For the laser flash measurement of semi-transparent zirconia it is in addition necessary to add a thin platinum layer on both sides of the ceramic coating, which were sputter coated before and after the EPD process with a thickness of about 5 μm. The thin Pt layer between sapphire and EPD coating prevents the laser beam penetration into the interior of the sample and ensures an effective and uniform absorption of the laser pulse. The thin Pt layer on the EPD coating surface serves as emission layer for measuring the temperature signal by the infrared detector. In addition, this opaque layer prevents the infrared detector from viewing into the sample interior and thus not giving an accurate temperature rise curve for the rear surface. Furthermore, for the EPD process the metal layer on the electrically non-conductive sapphire forms the necessary electrode.

The laser flash tests were performed in vacuum (between 10.5 and 10.4 mbar) from room temperature up to 1150 °C. In order to study sintering effects on the thermal conductivity, which are reported for conventional TBC systems,[17] the specimens were not only investigated in the as-sintered condition, but also after 100 h annealing in air at 1100 °C.

Further analysing tools were scanning electron microscopy (SEM, FEI XL30FEG), X-ray diffraction (XRD, Seifert 3003-TT) and differential scanning calorimetry (DSC, NETZSCH DSC 404).

3. Results and discussion

3.1. Phase transition during sintering

Before sintering the XRD spectra of specimen from suspensions *A* and *B* show peaks of tetragonal zirconia, of ZrN, and in addition very weakly of monoclinic zirconia (Fig. 4). Actually, the tetragonal and cubic phase can not be discerned by the available resolution of the XRD, but due to the composition of the YSZ (5 mol% Y_2O_3) the cubic phase is excluded. The as-received YSZ powder consists of tetragonal but also of a small volume fraction of monoclinic phase (Table 3). It may be hypothesized that the decreased volume fraction of the tetragonal phase found for the green coatings is due to the ball milling. Wang et al.[6] reported about such a transformation from tetragonal to monoclinic and explained it as a martensitic phase transformation induced by the fracture of YSZ grains.

After sintering in air at 1000 °C specimens from the suspensions *A* and *B* show pronounced peaks of monoclinic zirconia in addition to the ones of tetragonal zirconia (Fig. 4), while the peaks of ZrN disappeared. Within the detection limits of the XRD it can be stated that all ZrN transformed into zirconia. The specimen derived from suspension *A* has a lower volume fraction of the monoclinic phase than the one from suspension *B* (Table 3).

Table 3
Tetragonality of different specimens, derived from intensities of the diffraction peaks of monoclinic and tetragonal zirconia according to the formula by Toraya et al.[18]

Type	Volume fraction of the tetragonal phase relative to the monoclinic phase (%)
YSZ as-received	93.5
EPD coating from suspension *A*, green	92.8
From suspension *A*, sintered	54.4
From suspension *B*, green	88.0
From suspension *B*, sintered	54.5
From suspension *C*, green	92.0

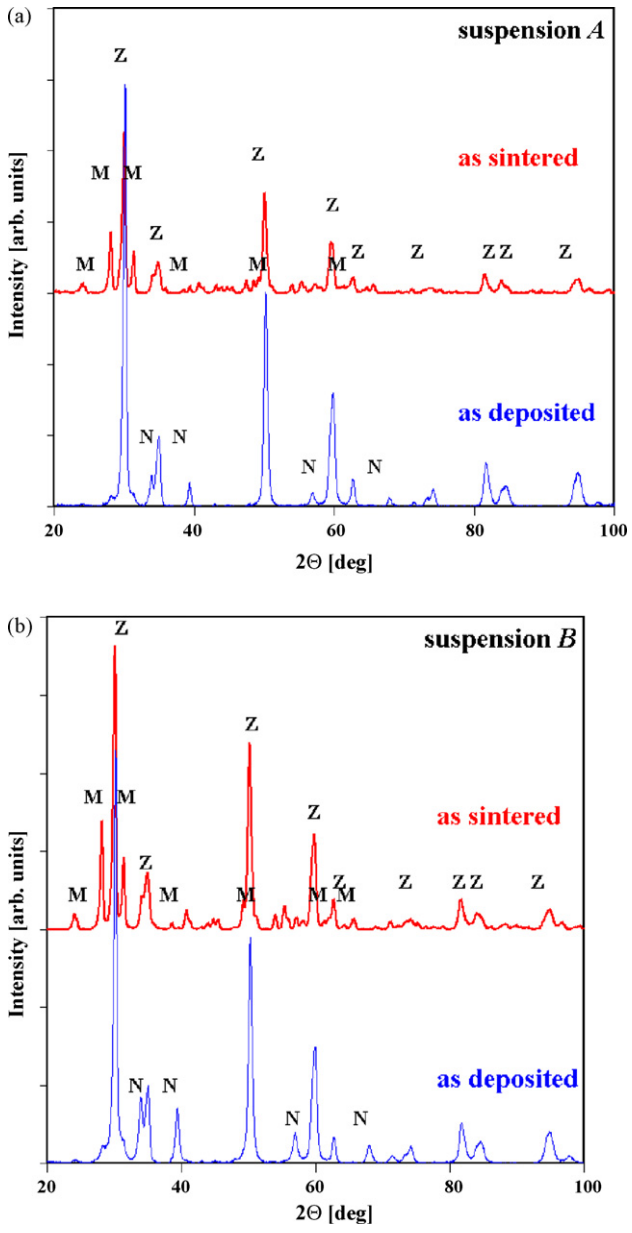

Fig. 4. XRD spectra of the ceramic coating of specimen from suspension *A* (a) and *B* (b) after EPD and after sintering in air at 1000 °C. Z: tetragonal zirconia, M: monoclinic zirconia, N: ZrN.

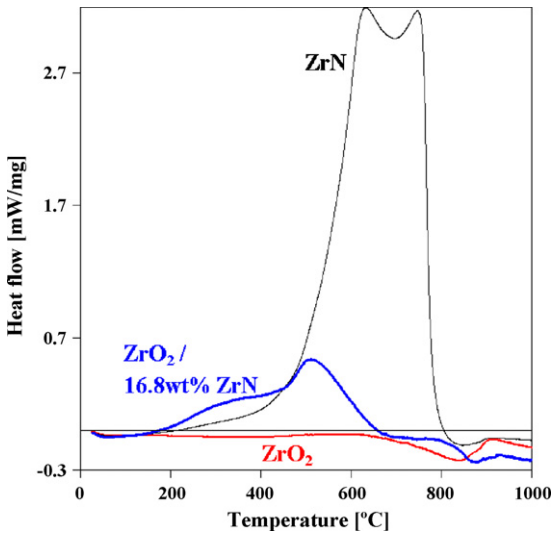

Fig. 5. DSC in air of the dried powder of suspension *B* (without the addition of the suspension stabilizers) in comparison with the one of the ZrN and zirconia powders as used for the suspension.

3.2. Thermal reactions

DSC was used to investigate the behavior of the YSZ/ZrN powder mix in air (flow rate 50 ml/min) in dependence on temperature (heating and cooling rate: 10 K/min). The DSC traces of the dried powder (before the addition of the suspension stabilizers) consist of several exothermal and endothermal peaks during heating (Fig. 5) and none during cooling. In order to understand the complex DSC spectrum, the starting powders YSZ and ZrN were measured as well.

YSZ shows during heating an endothermal peak around 850 °C. Since the YSZ powder contains not only tetragonal, but also monoclinic phase (see Table 3), this endothermal peak can be assigned to the monoclinic to tetragonal phase transformation in accordance with Suresh et al.[19] During cooling no more-transformation of the YSZ was observed indicating that the YSZ remained tetragonal. Zirconia with 5 mol% Y_2O_3 is more precisely called *t′*-zirconia, and shows in contrast to lower yttria content zirconia a reluctance to transform martensitically to the monoclinic phase during cooling.[20–22]

ZrN powder exhibits an exothermal double peak between 300 and 800 °C, which can be explained by a stepwise transformation from ZrN to ZrO_2. According to other authors[23,24] the transformation is not direct but intermediate species are formed, starting at 300 °C. The complete oxidation into ZrO_2 starts at 650 °C and at 950 °C only ZrO_2 was detected.[24]

With the thermal reactions of the starting powder the complex DSC spectrum of the powder mix can be understood. The superposition of the endothermal peak from the monoclinic to tetragonal transformation of YSZ and of the exothermal peak from the oxidation of ZrN results in a strong exothermal peak around 500 °C, a weaker exothermal peak around 800 °C and an endothermal peak around 830 °C. The zirconia resulting from the oxidation is not stabilized and the time at temperature is presumably too short to get a Y exchange with YSZ grains. Since the monoclinic to tetragonal phase transition of pure ZrO_2 is significantly higher (∼1200°) than for YSZ,[20] the oxidation of ZrN during the DSC will result in monoclinic ZrO_2. Therefore, at high temperatures the assumed phases are monoclinic zirconia from the oxidation and *t′*-zirconia from the YSZ and during cooling no further reaction will be observed.

Not yet explained is the exothermal peak of the powder mix around 300 °C. While YSZ and ZrN powders were investigated in the as-received condition, the powder mix has been milled in ethanol. Supposedly, even after drying OH groups exist on the surface of its grains, which may lead to the peak at this low temperature. DSC traces of green EPD coatings (not shown here), i.e. including the suspension stabilizers, are very similar to the ones of the powder mix, but have in addition another relatively sharp exothermal peak at

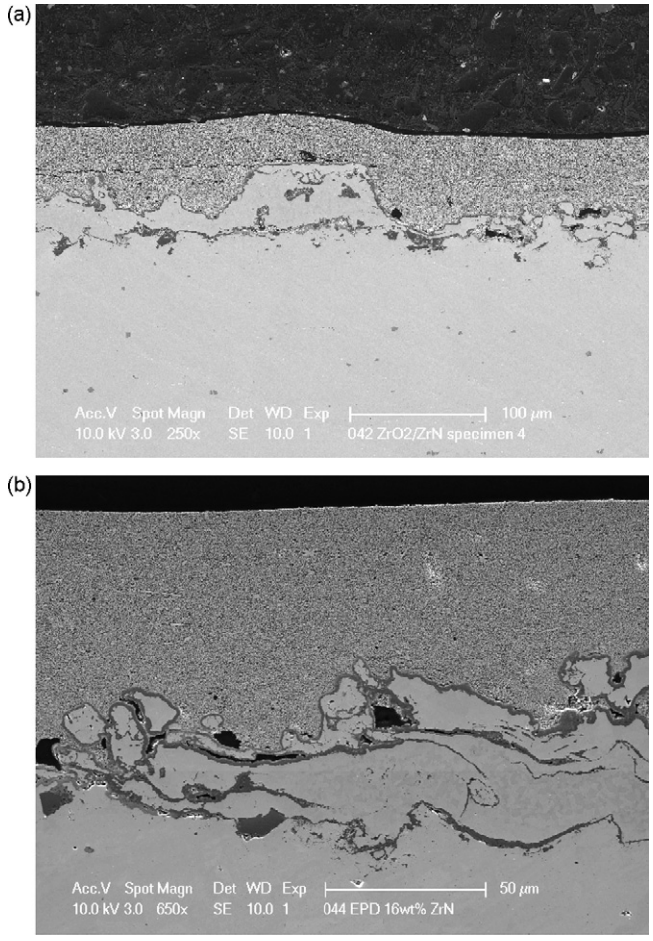

Fig. 6. Cross-section of EPD coatings on the IN600/NiCoCrAlY system, derived from suspensions *A* (a) and *B* (b), both with a deposition time of 60 s.

280 °C. This is attributed to the burning off of remains of the *n*-butylamine.

3.3. Microstructure

The cross-sections of EPD coatings on IN600/NiCoCrAlY substrates demonstrate that the EPD process levels out the surface roughness of the metal coating resulting in a smooth ceramic surface (Fig. 6). This may be attributed to the throwing power and the potential drop over the deposit of ethanol-based suspensions.[25] The EPD coatings appear homogenous and have only few agglomerates. Occasionally, cracks parallel to the surface can be observed. The rough and porous structure of the metal coating is also apparent in this figure. Due to the sintering in air a TGO has developed on the metal coating surfaces.

The more detailed view of Fig. 7 shows that the EPD coatings are relatively porous and that despite the low heat treatment temperature sintering has been achieved. The porosity seems to be comparable with the one of conventional EPD coatings sintered at 1200 °C.[13] Yet, it is obvious that suspension *B* resulted in a lower porosity than suspension *A*.

Close inspection of the micrographs (Fig. 7b and d) suggests that the ceramic coating is not single phased. On the grain surfaces and for the larger grains within the grains a darker grey phase can be discerned. Point analysis with EDX of the SEM indicates besides Zr and O the existence of Co, Cr and Fe in the regions of the darker phase. It may be speculated that these darker regions are additional oxides. However, no indication for this additional phase was found by XRD, which may be due to a too low volume fraction of this secondary phase or due to the possibility of being amorphous.

3.4. Thermal conductivity

Fig. 8 shows the thermal conductivity of specimens from suspensions *A*–*C*. At room temperature, the as-sintered EPD coatings have a very low thermal conductivity between 0.4 and 0.6 W/(m K) decreasing moderately with increasing temperature. Due to the lower density, the sintered EPD coating derived from suspension *A* has a lower thermal conductivity then the one from suspension *B*.

The coating derived from suspension *C* without addition of ZrN has a porosity of 38%.[13] Yet, despite the fact that it has a lower porosity than the one derived from suspension *B* (46%), it has a slightly lower thermal conductivity than the one from suspension *B*. Since their microstructural architecture is comparable, the difference in thermal conductivity may be related to the difference in yttria concentrations. With increasing yttria concentration the number of oxygen vacancies, at which the phonons are scattered, increases leading to a lower thermal conductivity.[26] Sintered coatings derived from suspensions with ZrN have a higher volume fraction of the monoclinic phase than coatings derived from suspension *C* (Table 3) and monoclinic zirconia has a lower amount of yttria and therefore a lower number of oxygen vacancies than tetragonal zirconia. Therefore, with similar porosity the coatings derived from suspensions with ZrN would have a higher thermal conductivity then the ones derived from suspension *C*. This effect seems to be so strong, that even with a lower porosity the coating from suspension *C* has a lower thermal conductivity than the one derived from suspension *B*.

Heat treatment for 100 h in air at 1100 °C significantly increases the thermal conductivity for all EPD coatings. It is noteworthy, that the specimen with the highest porosity not only has the lowest thermal conductivity, but also the smallest increase in thermal conductivity due to the heat treatment.

In comparison with commercially available thermal barrier coatings, like air plasma sprayed (APS) or electron beam physical vapour deposition (EB-PVD), the EPD coatings have remarkable low thermal conductivities. Values of about 0.8 W/(m K) for APS and 1.6 W/(m K) for EB-PVD coatings are reported for coatings in the initial state at room temperature, decreasing to 0.7 and 1.25 W/(m K), respectively, at 1150 °C[13,17] After corresponding heat treatment in air at 1100 °C for 100 h, these commercial coatings also showed a considerable increase in thermal conductivity to 1.3 W/(m K) for APS and 2.1 W/(m K) for EB-PVD thermal barrier coatings at room temperature, which are significantly higher values than for the EPD coatings. EPD allows therefore the fabrication of thermal barrier coatings with remarkably low thermal conductivity.

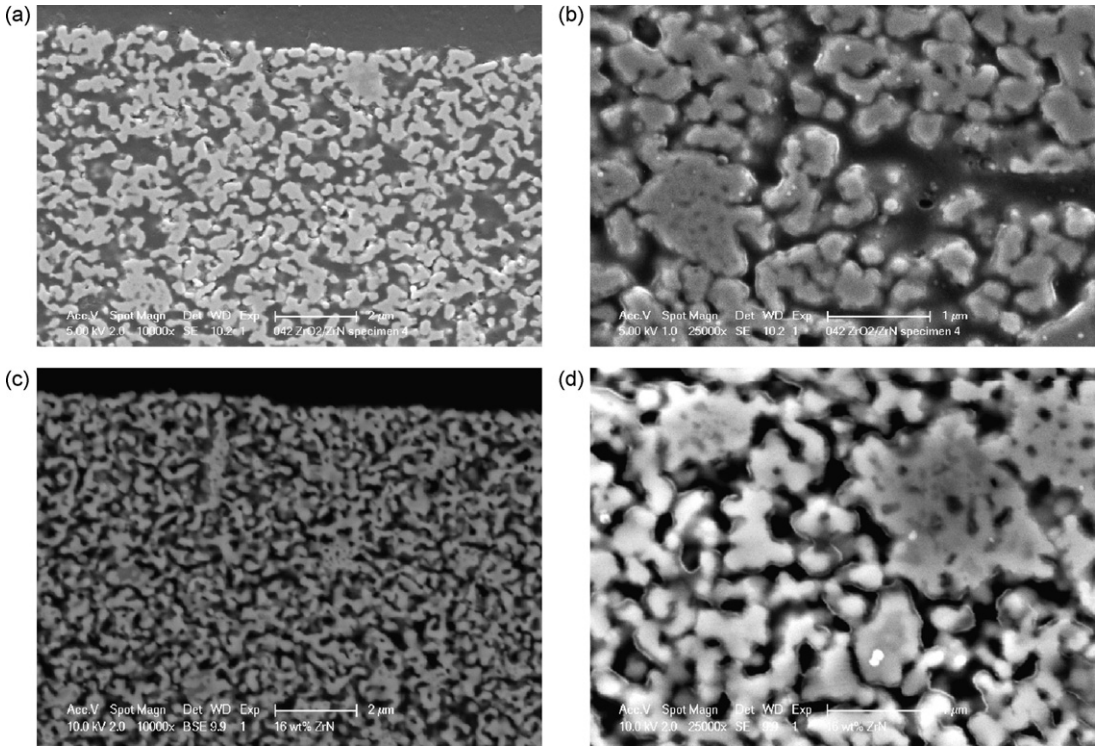

Fig. 7. Details of cross-sections of EPD coatings on the IN600/NiCoCrAlY system, derived from a suspension *A* (a and b) and *B* (c and d), both with a deposition time of 60 s.

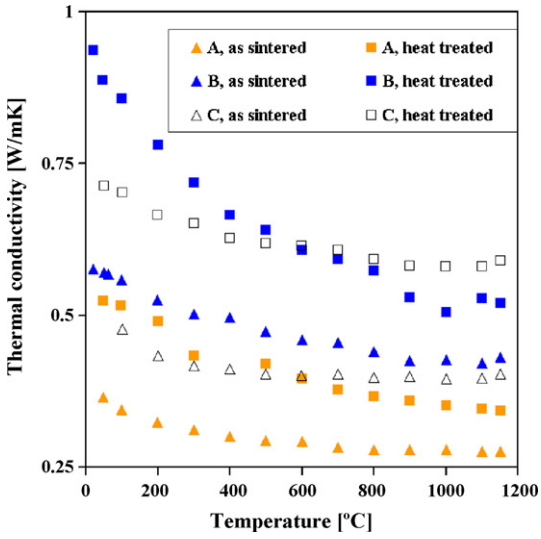

Fig. 8. Thermal conductivity in dependence on temperature during heating, in the as sintered condition and after 100 h heat treatment at 1100 °C in air of the two different EPD coatings with and without ZrN[13].

4. Conclusion

A stable ethanol based suspension with partially Y_2O_3 stabilized ZrO_2 and ZrN powder fractions has been prepared and successfully applied for EPD. With sintering in air at a remarkably low maximum temperature of 1000 °C porous ceramic coatings (≈0.1 mm thick) were obtained due to reaction bonding. The achieved homogenous microstructure is comparable with the one without reaction bonding but sintered at 1200 °C. Due to the throwing power of ethanol-based suspensions original surface roughness is levelled out resulting in a smooth surface. The resultant phases are tetragonal and monoclinic zirconia. The latter developed due to the oxidation of ZrN with a deficiency of stabilizing yttria. Further research with zirconia with higher yttria composition (for example fully stabilized zirconia) is worthwhile to investigate whether the monoclinic phase can be omitted. This would be advantageous due to detrimental volume changes of monoclinic-tetragonal transformations during in service temperature cycles to very high temperatures.

The thermal conductivity of the EPD coating proved to be remarkably low. However, annealing at 1100 °C increased the thermal conductivity drastically. Compared with thermal barrier coatings prepared by APS or EB-PVD, the reaction bonded EPD coatings have still superior thermal properties.

A drawback might be poor adherence, abrasive and corrosion resistance of EPD coatings, which still have to be investigated. Nevertheless, applications exist where the requirements to mechanical properties are less severe and cheaper thermal barrier coatings with lower thermal conductivity are desired.[27] Furthermore, if the aim is a low thermal conductivity and a good corrosion resistance, for example, a combination of EPD and APS is imaginable.

Acknowledgment

B. Baufeld acknowledges an individual Marie-Curie fellowship of the European Commission Nr. MEIF-CT-2005-010277.

References

1. Hannink, R. H. J., Kelly, P. M. and Muddle, B. C., Transformation toughening in zirconia-containing ceramics. *Journal of the American Ceramic Society*, 2000, **83**(3), 461–487.
2. Virkar, A. V., Role of ferroelasticity in toughening of zirconia ceramics. *Key Engineering Materials*, 1998, 153–154 (Zirconia Engineering Ceramics, 183–210).
3. Baither, D., Bartsch, M., Baufeld, B., Tikhonovsky, A., Foitzik, A., Rühle, M. and Messerschmidt, U., Ferroelastic and plastic deformation of t'-zirconia single crystals. *Journal of the American Ceramic Society*, 2001, **84**(8), 1755–1762.
4. Baufeld, B., Baither, D., Messerschmidt, U., Bartsch, M., Foitzik, A. and Rühle, M., Ferroelasticity of t'-zirconia, II. In situ straining in a high voltage electron microscope. *Journal of the American Ceramic Society*, 1997, **80**(7), 1699–1705.
5. Rao, D. U. K. and Subbarao, E. C., Electrophoretic deposition of magnesia. *American Ceramic Society Bulletin*, 1979, **58**(4), 467–469.
6. Wang, Z., Shemilt, J. and Xiao, P., Fabrication of ceramic composite coatings using electrophoretic deposition, reaction bonding and low temperature sintering. *Journal of the European Ceramic Society*, 2002, **22**(2), 183–189.
7. Kaya, C., Kaya, F., Atiq, S. and Boccaccini, A. R., Electrophoretic deposition of ceramic coatings on ceramic composite substrates. *British Ceramic Transactions*, 2003, **102**(3), 99–102.
8. van der Biest, O., Joos, E., Vleugels, J. and Baufeld, B., Electrophoretic deposition of zirconia layers for thermal barrier coatings. *Journal of Materials Science*, 2006, **41**, 8086–8092.
9. Wang, Z., Xiao, P. and Shemilt, J., Fabrication of composite coatings using a combination of electrochemical methods and reaction bonding process. *Journal of the European Ceramic Society*, 2000, **20**(10), 1469–1473.
10. Lu, F. and Lo, W., Degradation of ZrN films at high temperature under controlled atmosphere. *Journal of Vacuum Science & Technology A-Vacuum Surfaces and Films*, 2004, **22**(5), 2071–2076.
11. Mechnich, P. and Kerkamm, I., Reaction-bonded zirconia environmental barrier coatings for porous all-oxide ceramic matrix composites. In *Proceedings of the 31st International Conference on Advanced Ceramics and Composites*, 2007.
12. Onda, T., Yamauchi, H. and Hayakawa, M. "Effect of CoO doping on the sintering ability and mechanical properties of Y-TZP." *Designing, Processing and Properties of Advanced Engineering Materials*, 2004 (Pts 1 and 2), 265–268.
13. Baufeld, B., Rätzer-Scheibe, H. J. and van der Biest, O., Thermal and mechanical properties of zirconia coatings produced by electrophoretic deposition, In *Proceedings of the 31st International Conference on Advanced Ceramics & Composites*, Daytona Beach, Advanced Ceramic Coatings and Interfaces II, Ceramic Engineering and Science Proceedings, Volume 28, Issue 3, 2007, Jonathan Salem and Dongming Zhu, General Editors; Hua-Tay Lin and Uwe Schulz, Editors, p. 3–10.
14. Rätzer-Scheibe, H. J., Schulz, U. and Krell, T., The effect of coating thickness on the thermal conductivity of EB-PVD PYSZ thermal barrier coatings. *Surface and Coatings Technology*, 2006, **200**(18–19), 5636–5644.
15. Krell, T., PhD thesis: Thermische und thermophysikalische Eigenschaften von elektronenstrahlgedampften chemisch gradierten Al_2O_3/PYSZ-Wärmedämmschichten, *Rheinisch-Westfälische Technische Hochschule, Aachen*, 2000.
16. Schmitz, F., Hehn, D. and Maier, H. R., Evaluation of laser-flash measurements by means of numerical solutions of the heat conduction equation. *High Temperatures, High Pressures*, 1999, **31**(2), 203–211.
17. Rätzer-Scheibe, H.-J. and Schulz, U., The effects of heat treatment and gas atmosphere on the thermal conductivity of APS and EB-PVD PYSZ thermal barrier coatings. *Surface and Coatings Technology*, 2007, **201**(18), 7880–7888.
18. Toraya, H., Yoshimura, M. and Somiya, S., Calibration curve for quantitative-analysis of the monoclinic-tetragonal Zro2 system by X-ray-diffraction. *Journal of the American Ceramic Society*, 1984, **67**(6), C119–C121.
19. Suresh, A., Mayo, M. J. and Porter, W. D., Thermodynamics of the tetragonal-to-monoclinic phase transformation in fine and nanocrystalline yttria-stabilized zirconia powders. *Journal of Materials Research*, 2003, **18**(12), 2912–2921.
20. Scott, H. G., Phase relationships in the zirconia–yttria system. *Journal of Materials Science*, 1975, **10**(9), 1527–1535.
21. Rühle, M., Claussen, N. and Heuer, A. H. Microstructural studies of Y_2O_3-containing tetragonal ZrO2 polycrystals (Y-TZP). *Advances in Ceramics*, 1984, 12, 352–370 (Science and Technology of Zirconia II).
22. Chaim, R., Rühle, M. and Heuer, A. H., Microstructural evolution in a ZrO_2-12 wt% Y_2O_3 ceramic. *Journal of the American Ceramic Society*, 1985, **68**(8), 427–431.
23. Milosev, I., Strehblow, H. H., Gaberscek, M. and Navinsek, B., Electrochemical oxidation of ZrN hard (PVD) coatings studied by XPS. *Surface and Interface Analysis*, 1996, **24**(7), 448–458.
24. Wiame, H., Centeno, M.-A., Picard, S., Bastians, P. and Grange, P., Thermal oxidation under oxygen of zirconium nitride studied by XPS, DRIFTS, TG-MS. *Journal of the European Ceramic Society*, 1998, **18**(9), 1293–1299.
25. Anne, G., Neirinck, B., Vanmeensel, K., Van der Biest, O. and Vleugels, J., Throwing power during electrophoretic deposition. *Electrophoretic Deposition: Fundamentals and Applications II*, 2006, 187–191.
26. Schlichting, K. W., Padture, N. P. and Klemens, P. G., Thermal conductivity of dense and porous yttria-stabilized zirconia. *Journal of Material Science*, 2001, **36**, 3003–3010.
27. Aslan, M., Adam, J., Reinhard, B. and Veith, M., Preparation of thick zirconia coatings by spraying of colloidal suspensions. In *Proceedings of the 10th International Conference of the ECerS*, 2007.